PROPOSED EXPERIMENT FOR THE MEASUREMENT OF THE ANAPOLE MOMENT IN FRANCIUM

A. PEREZ GALVAN, D. SHENG , L. A. OROZCO†, AND THE FRPNC COLLABORATION *

Joint Quantum Institute, Department of Physics, University of Maryland and NIST, College Park, MD 20742, USA
†E-mail: lorozco@umd.edu
http://www.physics.umd.edu/rgroups/amo/orozco/index.html

This article presents a proposal of the FRPNC collaboration for a measurement of the anapole moment of the nucleus of francium using parity non-conservation as the signature in a hyperfine transition.

Keywords: Weak interaction; anapole moment; francium.

1. Introduction

Parity non conservation (PNC) is a unique signature of the weak interaction. Our current understanding of the weak interaction derives from the Standard Model of particle physics.[1,2]

The weak interaction produces two types of PNC effects in atoms: Nuclear spin independent and nuclear spin dependent.[3] Nuclear spin dependent PNC occurs in three ways:[4,5] An electron interacts weakly with a single valence nucleon (nucleon axial-vector current $A_n V_e$), the nuclear chiral current created by weak interactions between nucleons (anapole moment), and the combined action of the hyperfine interaction and the spin-independent Z^0 exchange interaction from nucleon vector currents ($V_n A_e$).[6–8]

This contribution presents a program to measure the anapole moment in a chain of francium isotopes. The ultimate goal is to further our understanding of the hadronic weak interaction, this is the delicate interplay of

*S. Aubin, (William and Mary), J. A. Behr (TRIUMF), G. Gómez, (San Luis Potosí), G. Gwinner (Manitoba), V. V. Fambaum (New South Wales), K. P. Jackson (TRIUMF), L. A. Orozco (Maryland), M. R. Pearson (TRIUNF), A. Pérez Galván (Maryland), D. Sheng (Maryland), G. D. Sprouse (TRIUNF), Y. Zhao (Shanxi)

Quantum Chromodynamics (QCD) with the weak interaction in the nucleus. The hadronic weak interaction is richer than the one in the leptonic sector as it occurs in the presence of the strong interaction which renormalizes the axial current. Its history starts shortly after the discovery in beta decay of parity violation[9–11] and continues to date with advances both in theory and experiment that are increasing our knowledge of this subject. These developments have brought with them the need to better understand QCD at low energy.

The recent review of Ramsey-Musolf and Page[12] shows the different avenues currently followed. There is an impressive theoretical development based on QCD that has produced an effective field theory (EFT) for the hadronic weak interaction.[13] The EFT relies on the important degrees of freedom of low-energy QCD. This EFT has connections with observables in a series of experiments proposed and/or currently under way. These include: $\overrightarrow{n} + p \rightarrow d + \gamma$, low energy $\overrightarrow{p} - p$ scattering, low energy $\overrightarrow{p} - \alpha$ scattering, spin rotation of polarized neutrons passing through hydrogen, measurement of spin rotation in helium, and measurement of the asymmetry in low energy photodisintegration of deuterium by polarized photons. The measurement of the seven observables form the future program for hadronic PV that is laid out in Ref.[14] The program involves performing a set of few-body measurements to determine the coefficients of the operators appearing in the EFT.[15] The situation of N-N parity violation, that is central to the low mass program, is not exempt from the small size of the weak interaction amplitudes relative to the strong interaction amplitudes at low energies. Theoretically the task to relate the underlying electroweak currents to low energy observables is complicated, as in this regime QCD is non-perturbative.[16]

The PNC measurements in heavier nuclei, ranging from ^{18}F to ^{133}Cs and ^{205}Tl, provide important input in the quest for understanding the hadron-hadron weak interaction. The interpretation of their results has relied on a meson exchange model that contains seven phenomenological meson-nucleon couplings, the model first proposed by Desplanques, Donoghue, and Holstein (DDH) in their seminal paper.[17] It has not been possible to obtain a self-consistent set of values for these couplings from existing measurements. The longest-range part of the interaction is dominated by the pion-nucleon coupling constant h_π. Values extracted from the pp and Cs anapole measurements[18,19] are consistent with each other, however they disagree by an order of magnitude with the value extracted from the circular polarization of the γ decay in ^{18}F and the anapole limit in ^{205}Tl.[20]

Despite the inconsistency, all numbers are still within the reasonable range defined by DDH.

The picture is complicated and it is important to encompass different approaches to elucidate the subtleties of the weak interaction in heavy nuclei. Erler and Ramsey-Musolf state in Ref.[15] that a study of the anapole moment provides a probe of the $\Delta S = 0$ hadronic weak interaction in nuclei. The disagreement between the results obtained with light mass systems compared to the anapole moment of Cs is puzzling. Haxton *et al.* suggest in Ref.[21] that strong interactions modify the isospin of weak meson-nucleon couplings in a nontrivial way.

2. Anapole measurement in francium

Zel'dovich postulated in 1957 that the weak interactions between nucleons would generate a parity violating, time reversal conserving moment called the anapole moment.[22] Flambaum and Khriplovich calculated the effect it would have in atoms.[5] Experiments in ^{205}Tl gave a limit for its value,[20] and it was measured for the first time with an accuracy of 14% through the hyperfine dependence of PNC in ^{133}Cs.[18,19] There are currently other efforts to study the anapole moment in Yt[23] and in polar molecules.[24]

The measurement strategy that we propose for the nuclear anapole moment in Fr relies on PNC. It looks for the direct excitation of the microwave electric dipole (E1), parity forbidden, transition between the ground state hyperfine levels in a chain of isotopes of Fr, the heaviest alkali atom. The E1 transition between hyperfine levels is parity forbidden, but becomes allowed by the anapole-induced mixing of levels of opposite parity. The general approach has been suggested in the past.[23,25–31] Many atoms, optically pumped to the appropriate magnetic sublevel, would be placed inside a microwave Fabry-Perot cavity and held in a blue-detuned dipole trap (see Fig. 1). The atoms would interact with the microwave field and with a Raman field generated by a pair of laser beams, in the presence of a static magnetic field. Confinement of the atoms to the node (anti-node) of the magnetic (electric) microwave field would drive only an E1 transition between hyperfine levels. The atoms would start in the lower hyperfine level, with the signal proportional to the population of atoms in the upper hyperfine level after the excitation. Interference with a Raman transition would produce a signal linear in the E1 transition, which is proportional to the anapole moment of the nucleus. (See Ref. [32] for details).

Parity violating atomic transitions are generated primarily by the exchange of weak neutral currents between electrons and nucleons. Assuming

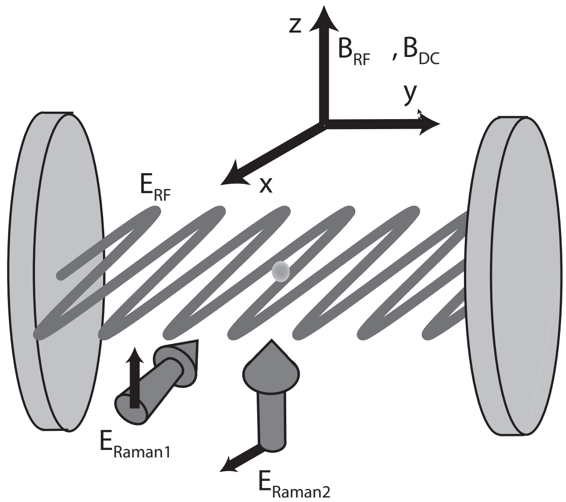

Fig. 1. Schematic setup of the proposed apparatus, adapted from Ref.[32] The dipole trap is not shon and the Raman beams (thick arrows [gray] indicate their propagation and thin [black] arrows state their polarization).

an infinitely heavy nucleon without radiative corrections, the hamiltonian is:[33]

$$H = \frac{G}{\sqrt{2}}(\kappa_{1i}\gamma_5 - \kappa_{nsd,i}\boldsymbol{\sigma_n} \cdot \boldsymbol{\alpha})\delta(\mathbf{r}), \tag{1}$$

where $G = 10^{-5}$ m_p^{-2} is the Fermi constant, m_p is the proton mass, γ_5 and α are Dirac matrices, $\sigma_\mathbf{n}$ are Pauli matrices, and κ_{1i} and $\kappa_{nsd,i}$ (nuclear spin dependent) with $i = p, n$ for a proton or a neutron are constants of the interaction. At the tree level $\kappa_{nsd,i} = \kappa_{2i}$, and in the standard model these constants are given by $\kappa_{1p} = 1/2(1-4\sin^2\theta_W)$, $\kappa_{1n} = -1/2, \kappa_{2p} = -\kappa_{2n} = \kappa_2 = -1/2(1-4\sin^2\theta_W)\eta$, with $\sin^2\theta_W \sim 0.23$ the Weinberg angle, and $\eta = 1.25$. κ_{1i} (κ_{2i}) represents the coupling between nucleon and electron currents when the electron (nucleon) is the axial vector.

In an atom, we must add the contribution from Eq. 1 for all the nucleons. It is convenient to work in the approximation of a shell model with a single valence nucleon of unpaired spin. The second term of Eq. 1 is nuclear spin dependent and due to the pairing of nucleons its contribution has smaller dependence on Z. The result for this second term is:[34]

$$H^{nsd,i}_{PNC} = \frac{G}{\sqrt{2}}\frac{K\boldsymbol{I}\cdot\boldsymbol{\alpha}}{I(I+1)}\kappa_{nsd}\delta(r), \tag{2}$$

where $K=(I+1/2)(-1)^{I+1/2-l}$, l is the nucleon orbital angular momentum, and I is the nuclear spin. The terms proportional to the anomalous magnetic moment of the nucleons and the electrons have been neglected.

The interaction constant is given now by:[34]

$$\kappa_{nsd,i} = \kappa_{a,i} - \frac{K-1/2}{K}\kappa_{2,i} + \frac{I+1}{K}\kappa_{Q_W}, \tag{3}$$

where $\kappa_{2,p} = \kappa_{2,n} = -(1/2)1.25(1-4\sin\theta_W{}^2) \sim -0.05$ within the tree level approximation; and we have two radiative corrections, the effective constant of the anapole moment $\kappa_{a,i}$, and κ_{Q_W} that is generated by the nuclear spin independent part of the electron nucleon interaction together with the hyperfine interaction. Nuclear calculations give[34]

$$\kappa_{a,i} = \frac{9}{10} g_i \mu_i \frac{\alpha \mathcal{A}^{2/3}}{m_p \tilde{r_0}}, \qquad \kappa_{Q_W} = -\frac{1}{3}\left(\frac{Q_W}{\mathcal{A}}\right)\mu_N \frac{\alpha \mathcal{A}^{2/3}}{m_p \tilde{r_0}}, \tag{4}$$

where α is the fine structure constant, μ_i and μ_N are the magnetic moment of the external nucleon and of the nucleus, respectively, in nuclear magnetons, $\tilde{r_0}=1.2$ fm is the nucleon radius, $\mathcal{A} = \mathrm{Z}+\mathrm{N}$, the weak charge Q_W is approximately equal to the number of neutrons N,[3] and g_i gives the strength of the weak nucleon-nucleon potential with $g_p \sim 4$ for protons and $0.2 < g_n < 1$ for neutrons.[33] Since both κ_a and κ_{Q_W} scale as $\mathcal{A}^{2/3}$, the interaction is stronger in heavier atoms. The anapole moment is the dominant contribution to the interaction in heavy atoms, for example in ^{209}Fr, $\kappa_{a,p}/\kappa_{Q_W} \simeq 15$. $\kappa_{nsd,i} = \kappa_{a,i}$ is assumed unless stated otherwise for the rest of the proposal.

The anapole moment is defined by

$$\mathbf{a} = -\pi \int d^3 r r^2 \mathbf{J}(\mathbf{r}), \tag{5}$$

with $\mathbf{J}$ the nuclear current density. The anapole moment in francium arises from the weak interaction between the valence nucleons and the core. By including weak interactions between nucleons in their calculation of the nuclear current density, Flambaum *et al.*[5] estimate the anapole moment from Eq. 5 of a single valence nucleon to be

$$\mathbf{a} = \frac{1}{e}\frac{G}{\sqrt{2}}\frac{K\boldsymbol{j}}{j(j+1)}\kappa_{a,i} = C^{an}\boldsymbol{j}, \tag{6}$$

where j is the nucleon angular momentum. For the case of a single valence nucleon these values correspond to the nuclear values. Flambaun, Khriplovich and Shushkov[5,35,36] estimated the magnitude of the anapole

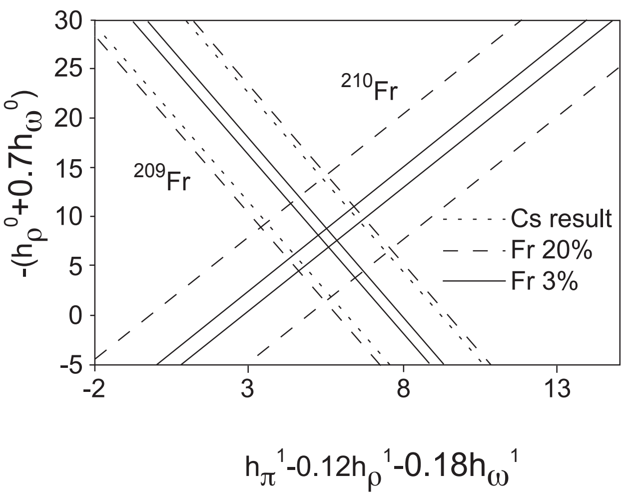

Fig. 2. Range of meson coupling parameters for the expected values of the anapole moment for two Fr isotopes 209 and 210.

moments of various nuclei, demonstrating the $\mathcal{A}^{2/3}$ scaling under the valence nucleon assumption. This is for a shell model with a single valence nucleon carrying all the angular momentum. Flambaum and Murray[34] took the parametrization of DDH[17] and found the corresponding coupling constants associated with the anapole moment of Cs under these assumptions.

Figure 2 shows the possible results based on the model with a single valence nucleon or the vectorial addition of the proton and the neutron in the outer shell that induce the anapole moment. Testing the striking predictions of this simple model near closed shells, and its even-odd staggering behavior, could clarify such a phenomenological treatment to allow the extraction of the weak hadronic physics. If the prediction fails, then it would provide necessary information as input to more sophisticated shell model treatments to extract the physics. This simple approach gives results consistent with the more detailed calculations of Ref.[21] and confirms their assessment that new anapole measurements in odd-neutron nuclei would have great impact, defining a band of the weak meson-nucleon coupling plane roughly perpendicular to the Cs and Tl bands . The model of Fig. 2 predicts that measuring the anapole moment on two isotopes gives an almost orthogonal crossing in the two linear combinations of the meson coupling constants from the DDH model. The values plotted in this figure are slightly different from the ^{133}Cs band in Ref.[6] as a different choice of values of the "best paramenters" were used.

3. Method for the anapole moment measurement

We calculate the transition amplitude for ^{209}Fr between the hyperfine level F=4, m=0 to F=5, m=-1 with a microwave electric field of 476 V/cm oscillating along the x-axis and a static magnetic field of 1553 Gauss along the z-axis, and with the total anapole moment (κ_a) resulting from the vectorial addition of the valence proton and neutrons in ^{209}Fr as 0.45. We obtain[32]

$$A_{E1}/h = \Omega_{E1} = \langle \bar{f}| - e\mathbf{E}\cdot\mathbf{r}|\bar{i}\rangle/h = 0.01i\left[\frac{E}{476\mathrm{V/cm}}\right]\left[\frac{\kappa_a}{0.45}\right] \quad \mathrm{rad/s.} \tag{7}$$

Once the atoms are in the dipole trap we would optically pump them into a single Zeeman sublevel to prepare a coherent superposition of the hyperfine ground states with a Raman pulse of duration t_R. We would drive the E1 transition with the cavity microwave field for a fixed time t_{E1}, and then measure the population in the upper hyperfine level (normalized by the total number of atoms N) through a cycling transition. At the end of each sequence the excited state population is given by

$$\Xi_\pm = N|c_e|^2 = N\sin^2\left(\frac{\Omega_R t_R}{2} \pm \frac{\Omega_{E1}t_{E1}}{2}\right), \tag{8}$$

where c_e is the upper hyperfine amplitude, Ω_R and Ω_{E1} are the respective Rabi frequencies of the Raman and E1 transition, and the sign depends on the handedness of the coordinate system defined by the external fields as explained below. For a $\pi/2$ Raman pulse (or a 50-50 coherent superposition) and small Ω_{E1} this equation becomes

$$\Xi_\pm = N|c_e|^2 \sim N\left(\frac{1}{2} \pm \frac{\Omega_{E1}t_{E1}}{2}\right). \tag{9}$$

The second term contains the PNC signal (E1 transition) that becomes linear through the interference with the Raman transition. We measure the population transfer for both signs and define the signal, proportional to κ_a, as

$$\mathcal{S} = \Xi_+ - \Xi_- = N\Omega_{E1}t_{E1}. \tag{10}$$

The atoms (located at the origin as indicated in Fig. 1) are prepared in a particular Zeeman sublevel $|F, m\rangle$. We apply a static magnetic field $\mathbf{B} = B\hat{\mathbf{z}}$. The atoms are excited by an standing-wave microwave electric field $\mathbf{E}(t) = E\cos(\omega_m t + \psi)\cos(k_m y)\hat{\mathbf{x}}$. The microwave frequency ω_m is tuned to the Zeeman-shifted hyperfine transition frequency ω_0. The microwave magnetic field $\mathbf{M}$ is deliberately aligned along $\mathbf{B}$; since (for a perfect standing wave) $\mathbf{M}$ is out of phase with $\mathbf{E}$, we thus have $\mathbf{M}(t) = M\sin(\omega_m t + \psi)\sin(k_m y)\hat{\mathbf{z}}$, with $M = E$ in cgs units. Proper alignment of $\mathbf{M}$ and positioning of the standing-wave node is critical for suppressing systematic effects and line-broadening mechanisms. The Raman transition is driven by two plane-wave optical fields, $\mathbf{E}_{R1}(t) = E_{R1}\cos(\omega_R t + \phi_R)\hat{\mathbf{x}}$ and $\mathbf{E}_{R2}(t) = E_{R2}\cos((\omega_R + \omega_m)t + \phi_R)\hat{\mathbf{z}}$. We assume that the Raman carrier frequency ω_R is detuned sufficiently far from optical resonance that only the vector part of the Raman transition amplitude ($\mathbf{V} \propto i\mathbf{E}_{R1} \times \mathbf{E}_{R2}$) is non-negligible.[37]

The various electric and magnetic fields of the apparatus define a coordinate system related to the measured rate $\Xi_\pm$. The transition rate $\Xi_\pm$ depends on three vectors: The polarization of the E1 transition, the polarization of the Raman transition ($\mathbf{V}$), and the static magnetic field $\mathbf{B}$ which defines magnetization of the atoms. We combine these three vectors to produce the pseudoscalar $\mathbf{i}(\mathbf{E} \times (\mathbf{E}_{R1} \times \mathbf{E}_{R2}))\cdot\mathbf{B}$ proportional to the measured quantity. We include no discussion about systematic effects in this contribution, as this is presented at great length in Ref.[32]

The measurement of the upper hyperfine state population collapses the state of each atom into one of the two hyperfine levels. The collapse distributes the atoms binomially between the two hyperfine levels and leads to an uncertainty in the measured excited state fraction called projection noise.[38] The projection noise is $\mathcal{N}_P = \sqrt{N|c_e|^2(1 - |c_e|^2)}$. For a projection noise limited measurement, the signal-to-noise ratio is

$$\frac{\mathcal{S}}{\mathcal{N}_P} = 2\Omega_{E1} t_R \sqrt{N}, \tag{11}$$

With 10^6 francium atoms, which combined with Ω_{E1} given by Eq. 7 for a field of 476 V/cm and $\kappa_a = 0.45$ in $t_R = 1$ s, Eq. 11 gives a signal-to-noise ratio of 20. Another way to state the same is that with 300 atoms we will need 10^4 cycles of t_R duration to reach a 3% statistical uncertainty.

There are other sources of noise such as the photon shot noise, that scales as $\sqrt{N|c_e|^2}$, or technical noise that is independent of c_e. About a 50-50 initial superposition of states maximizes the signal-to-noise ratio when we include shot noise and some technical noise beyond projection noise.

4. Fr production requirements

Francium is expected to have an anapole PNC effect a factor of ten times larger than cesium.[39] Fr is, however, an unstable element and it is necessary to use an accelerator to produce it in a fusion or fission reaction[40] or take from the decay process of thorium.[41] The program presented in this contribution relies on the laser trapping an cooling techniques that can capture enough atoms for performing the measurement. The most efficient MOT Fr trap[40] had an overall efficiency of a few percent; so to capture 10^6 in the dipole trap it would be good to have production rates in excess of 10^8 per second or larger with lifetimes of tens of seconds in the MOT. We expect that the developing actinite source at TRIUMF in Vancouver, Canada will be able to achieve that production rate for various isotopes both in the neutron rich and neutron deficient side. Other accelerators existing or in planning stages should also achieve comparable or better numbers. The program of PNC studies for nuclear hadronic weak interaction will greatly benefit from the Fr experiments and its success hinges on good Fr production.

5. Acknowledgments

Work supported by the National Science Foundation of the USA.

References

1. S. Weinberg, *Phys. Rev. Lett.* **19**, p. 1264 (1967).
2. A. Salam, *Gauge Unification of Fundamental Forces*, in *Elementary Particle Theory: Relativistic Groups and Analyticity (8th Nobel Symp.)*, ed. N. Svartholm (Almqvist and Wicksell, Amsterdam, 1968), Amsterdam, p. 367.
3. M.-A. Bouchiat and C. Bouchiat, *Rep. Prog. Phys.* **60**, p. 1351 (1997).
4. Y. B. Zel'dovich, *Sov. Phys.-JETP* **9**, p. 682 (1959).
5. V. V. Flambaum, I. B. Khriplovich and O. P. Sushkov, *Phys. Lett. B* **146**, p. 367 (1984).
6. W. C. Haxton and C. E. Wieman, *Annu. Rev. Nucl. Part. Sci.* **51**, p. 261 (2001).
7. W. R. Johnson, M. S. Safronova and U. I. Safronova, *Phys. Rev. A* **67**, p. 062106 (2003).
8. J. S. M. Ginges and V. V. Flambaum, *Phys. Rep.* **397**, p. 63 (2004).
9. C. S. Wu, E. Ambler, R. W. Hayward, D. D. Hoppes and R. P. Hudson, *Phys. Rev.* **105**, p. 1413 (1957).
10. J. I. Friedman and V. L. Telegdi, *Phys. Rev.* **106**, p. 1681 (1957).
11. R. L. Garwin, L. M. Lederman and M. Weinrich, *Phys. Rev.* **105**, p. 1415 (1957).
12. M. J. Ramsey-Musolf and S. A. Page, *Ann. Rev. Nucl. Part. Sci.* **56**, p. 1 (2006).
13. S.-L. Zhu, C. Maekawa, B. Holstein, M. J. Ramsey-Musolf and U. van Kolck, *Nucl. Phys. A* **748**, p. 435 (2005).

14. B. R. Holstein, *Intersections of Particle and Nuclear Physics: 8th Conference, AIP Conf. Proc.* **698**, p. 176 (2003).
15. J. Erler and M. J. Ramsey-Musolf, *Prog. Nucl. Part. Phys.* **54**, p. 351 (2005).
16. W. M. Snow, *Eur. Phys. J. A* **24 s1**, p. 119 (2005).
17. B. Desplanques, J. F. Donoghue and B. R. Holstein, *Ann. Phys. (N.Y.)* **124**, p. 449 (1980).
18. C. S. Wood, S. C. Bennett, D. Cho, B. P. Masterson, J. L. Roberts, C. E. Tanner and C. E. Wieman, *Science* **275**, p. 1759 (1997).
19. C. S. Wood, S. C. Bennett, J. L. Roberts, D. Cho and C. E. Wieman, *Can. J. Phys.* **77**, p. 7 (1999).
20. P. A. Vetter, D. M. Meekhof, P. K. Majumder, S. K. Lamoreaux and E. N. Fortson, *Phys. Rev. Lett.* **74**, p. 2658 (1995).
21. W. C. Haxton, C. P. Liu and M. J. Ramsey-Musolf, *Phys. Rev. C* **65**, p. 045502 (2002).
22. Y. B. Zel'dovich, *Sov. Phys.-JETP* **6**, p. 1184 (1958).
23. D. Budker, *Parity Noncoservation in Atoms*, in *WEIN 98, Physics Beyond the Standard Model*, eds. P. Herczeg, C. M. Hoffman and H. V. Klapdor-Kliengrethaus (World Scientific, Singapore, 1998), Singapore, p. 418.
24. D. P. DeMille, S. B. Cahn, D. Murphree, D. A. Rahmlow and M. G. Kozlov, **arXiv:0708.2925** (2007).
25. C. E. Loving and P. G. H. Sandars, *J. Phys. B* **10**, p. 2755 (1977).
26. V. G. Gorshkov, V. F. Ezhov, M. G. Kozlov and A. I. Mikhailov, *Sov. J. Nucl. Phys.* **48**, p. 867 (1988).
27. V. E. Balakin and S. I. Kozhemyachenko, *JETP Lett.* **31**, p. 297 (1980).
28. V. N. Novikov and I. B. Khriplovich, *JETP Lett.* **22**, p. 74 (1975).
29. E. A. Hinds and V. W. Hughes, *Phys. Lett. B* **67**, p. 487 (1977).
30. E. G. Adelberger, T. A. Traino, E. N. Fortson, T. E. Chupp, D. Holmgren, M. Z. Iqbal and H. E. Swanson, *Nuc. Instr. and Meth.* **179**, p. 181 (1981).
31. E. N. Fortson, *Phys. Rev. Lett.* **70**, p. 2383 (1993).
32. E. Gomez, S. Aubin, L. A. Orozco, G. D. Sprouse and D. DeMille, *Phys. Rev. A* **75**, p. 033418 (2007).
33. I. B. Khriplovich, *Parity Non-Conservation in Atomic Phenomena* (Gordon and Breach, New York, 1991).
34. V. V. Flambaum and D. W. Murray, *Phys. Rev. C* **56**, p. 1641 (1997).
35. V. V. Flambaum and I. B. Khriplovich, *Sov. Phys. JETP* **52**, p. 835 (1980).
36. O. P. Sushkov, V. V. Flambaum and I. B. Khriplovich, *Sov. Phys. JETP* **60**, p. 873 (1984).
37. D. DeMille and M. G. Kozlov, *arXiv:* **physics**, p. 9801034 (1998).
38. W. M. Itano, J. C. Begquist, J. J. Bollinger, J. M. Gilligan, D. J. Heinzen, F. L. Moore, M. G. Raizen and D. J. Wineland, *Phys. Rev. A* **47**, p. 3554 (1993).
39. V. A. Dzuba, V. V. Flambaum and O. P. Sushkov, *Phys. Rev. A* **51**, p. 3454 (1995).
40. E. Gomez, L. A. Orozco and G. D. Sprouse, *Rep. Prog. Phys.* **69**, p. 79 (2006).
41. Z.-T. Lu, K. L. Corwin, K. R. Vogel, C. E. Wieman, T. P. Dinneen, J. Maddi and H. Gould, *Phys. Rev. Lett.* **79**, p. 994 (1997).